

UNIVERSITY OF EXETER
MPHYS PROJECT

**Thermoelectric Efficiency of
Zero-dimensional Nanocomposites**

Author:
Callum VINCENT

Supervisor:
Prof. G. P. SRIVASTAVA

April 2015

Abstract

Thermoelectrics are currently limited by their heat to electric conversion efficiency. If their efficiency can be improved 3x then a wide array of technological applications can be developed. Nanocomposite structuring is a potential technique for achieving this. We utilise an effective medium approximation to calculate the thermoelectric efficiency of a zero-dimensional SiGe nanocomposite. We find that silicon spheres of 10nm diameter densely packed in a germanium host medium, increases the thermoelectric efficiency 4x compared to bulk SiGe. This gives a good indication that further theoretical and experimental research should be conducted.

Contents

I Introduction	1
1.1 Motivation	1
1.2 Approach	2
1.3 Investigation	4
II Background Theory	4
2.1 Boltzmann Equation	5
2.2 Phonons	5
2.3 Debye Isotropic Continuum Model	7
2.4 Phonon Thermal Conductivity	8
2.5 Fermi Level	9
2.6 Electrical Conductivity	12
2.7 Electrical Thermal Conductivity	13
III Specific Theory	14
3.1 Thermoelectric Effect & Seebeck Coefficient	14
3.2 Thermoelectric Efficiency	17
3.3 Nanocomposites	17
3.4 Effective Medium Approximation	20
IV Results and Analysis	21
V Conclusion and Future Work	25
5.1 Future Work	25
5.2 Online repository	25
A Tools and Software	28
B Physical Data	28

I Introduction

1.1 Motivation

Energy and its use defines human society. Throughout history we have seen an upwards trend of energy consumption and with it we transform our environment and our lives.

Thermoelectric materials have the potential to revolutionise our energy harvesting methods due to their ability to convert heat directly into electricity. This potential has motivated decades of research, resulting in; radioisotope thermonuclear generators, solid state refrigerators and precise thermal control systems.

The main limitation of thermoelectric materials is their heat to electricity conversion efficiency. In modern applications, this is approximately 7% [1], roughly 4x lower than what is currently possible for internal combustion engines [2].

Recent advances in nano-fabrication have facilitated the development of new nanocomposite materials. Closely resembling metamaterials; nanocomposites are typically periodic arrays of nanoscale sheets, wires or particles. In 2001, it was shown that layering thin-films of thermoelectric materials gave a 2.4x increase in the thermoelectric figure of merit ZT [3]; a key parameter in the conversion efficiency discussed above.

If ZT can be increased from 1 to 3, an efficiency comparable to combustion engines could be attained in typical thermoelectric systems [4]. This would open up a wide array of applications such as: solar thermoelectric panels [5], exhaust heat recovery systems [6] and high reliability refrigeration systems [7].

It is therefore the goal of this project to understand how nanocomposite structuring effects the electrical and thermal properties of thermoelectric materials and whether a $ZT > 3$ can be achieved.

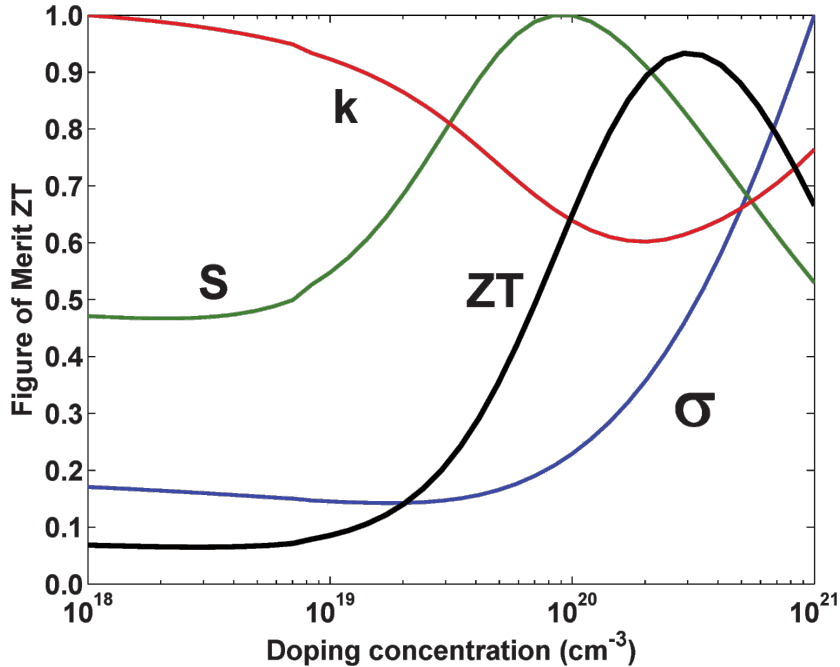


Figure 1: Normalised thermoelectric properties *versus* doping concentration at 300 K for n-type Si₈₀Ge₂₀ [8]. Variables defined as follows: S Seebeck coefficient, σ electrical conductivity, k thermal conductivity and ZT the thermoelectric figure of merit (proportional to conversion efficiency). The interrelationships between the variables gives a maximum ZT for a heavily doped semiconductor.

1.2 Approach

Thermoelectricity requires a compromise between 3 variables; S the Seebeck coefficient, σ the electrical conductivity and k the thermal conductivity. The thermoelectric figure of merit ZT and ultimately the conversion efficiency, is maximised when both S and σ are much greater than k . This is well shown in Figure 1, where a decreasing k and increasing σ produce a maximum in ZT .

The problem therefore lies in the complex interplay between these 3 variables; how do we disentangle their relationships and produce a positive effect on ZT ?

In the *CRC Handbook of Thermoelectrics* [9], G. A. Slack proposes a mechanism for enhancing ZT, the phonon glass electron crystal (PGEC). In a PGEC, the material is structured to restrict phonon propagation (PG), but enhance electron propagation (EC). If these two effects are independent, then the resultant increase in electrical conductivity and decrease in thermal conductivity will boost ZT, as in Figure 1.

In 1993, Hicks and Dresselhaus theoretically showed that a nanocomposite of closely packed nanoscale cylinders had the potential to significantly increase ZT [10]. We interpreted their findings to be in agreement with the PGEC concept; the cylinder boundaries are scattering phonons, whilst leaving the electrons unaffected. Therefore nanocomposite structuring may offer a possible technique for developing a PGEC material.

As a relatively new field, nanocomposites and its conceptual framework is still young and in development. In the context of thermoelectrics, theories for S , σ and k all need to be explored. We hypothesised that the main reason for the increase of ZT in nanocomposite structuring, is the scattering of phonons. So for our project, we decided to focus on k , specifically the phononic contribution k_{ph} .

Of the literature reviewed, two theories for k_{ph} were of note, the effective medium approximation (EMA) [11] and the phonon hopping model (PHM) [12]. The EMA considers a homogeneous host material whose phonon thermal conductivity is perturbed by a regularly arranged nanostructure. Whereas the PHM considers a linear chain of host atoms regularly perturbed by nanoparticles and calculates the probability of a phonon hopping past or interacting with these nanoparticles. We evaluated both models in detail and decided that the PHM neglected crucial thermoelectric properties, so we adopted the EMA for our calculations.

Our final consideration is which nanocomposite structure to investigate. Originally, we had planned to test multiple structures and compare their effects. However, as we were studying the EMA theory, it became clear that the optimum structure would have a high density of interfaces, with maximal gaps between these interfaces. This made closely packed spheres an ideal choice, as there is minimal contact between the spheres and a large surface area exposed to the host material. This structure is illustrated in Figure 2.

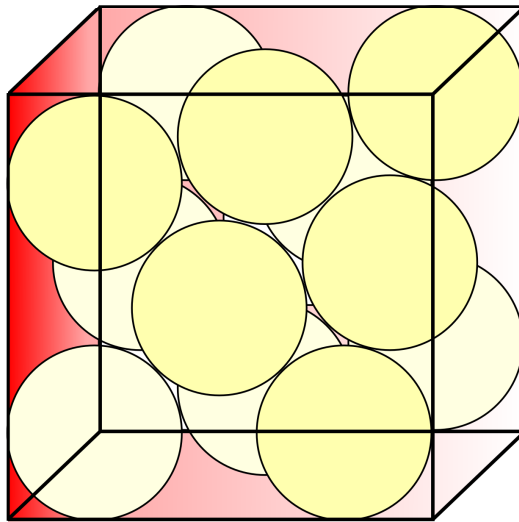


Figure 2: Zero-dimensional nanocomposite structure. Nanoscale spheres are densely packed with a homogeneous host material filling the voids. A temperature gradient is shown, to illustrate use as a thermoelectric.

1.3 Investigation

With the components discussed in the previous section, we have a clear plan of action. We must start by defining the non-equilibrium transport dynamics as in Section 2.1. We then need a detailed description of phonons and electrons as is given in Section 2.2 and Section 2.6. Finally, we must apply these results to the EMA model and define the figure of merit ZT for our chosen nanocomposite structure, as is done in Section 3.2 and Section 3.4. Our final results pull together all of this, to present a first principles theory of thermoelectric efficiency in a zero-dimensional SiGe nanocomposite.

II Background Theory

All the theories discussed in this report are transport processes. Therefore fundamental to them all are the non-equilibrium statistical mechanics of their quasiparticles.

2.1 Boltzmann Equation

The Boltzmann equation describes the statistical behaviour of a thermodynamic system of particles not in thermodynamic equilibrium and its general definition is [13]:

$$\frac{f}{t} = \left(\frac{\partial f}{\partial t} \right)_{\text{force}} + \left(\frac{\partial f}{\partial t} \right)_{\text{diff}} + \left(\frac{\partial f}{\partial t} \right)_{\text{coll}} \quad (1)$$

where $\frac{\partial f}{\partial t}$ is the time dependence of the distribution function of the particles f , the “force” term represents external forces on the particles, the “diff” term is the diffusion of particles through the system and the “coll” term represents forces acting between particles in collisions.

From this general definition we can find how a particular system of particles or quasiparticles are distributed across a material and therefore find their average motion. We use this in the electrical conductivity σ (Section 2.6) and phonon thermal conductivity k_{ph} (Section 2.4) derivations.

So we have a way of finding the distribution of our quasiparticles, but what exactly are the quasiparticles we are dealing with? And how are they important in the context of thermoelectrics?

2.2 Phonons

A phonon is the quantisation of vibrational motion of a lattice of atoms at a single frequency, known as a normal mode [13]. These phonons are quasi-particles, free to move around the crystal lattice and they are distributed according to the Bose-Einstein distribution [13]:

$$\bar{n} = \frac{1}{e^{(\hbar\omega)/kT} - 1} \quad (2)$$

where \bar{n} is the probability of a phonon existing with energy $\hbar\omega$ at temperature T . This distribution is shown in Figure 3

Phonons are carriers of acoustic and thermal energy through a material. They follow two types of dispersion; optical and acoustic. These two

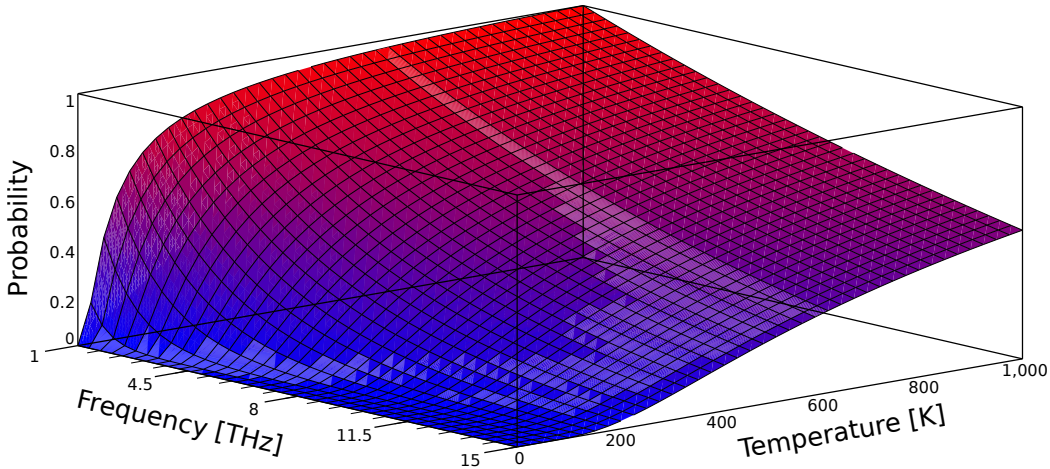


Figure 3: Probability of phonon occupancy *versus* phonon frequency and temperature, computed from the Bose-Einstein distribution [13]. Frequencies at and above 15THz represent optical phonons.

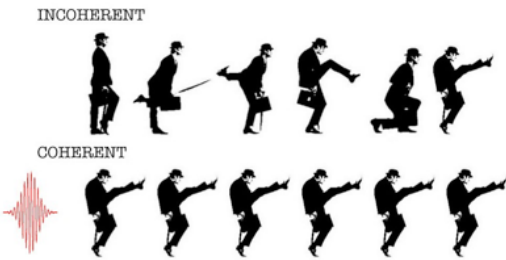


Figure 4: An incoherent walk, contrasted with a coherent walk. For the coherent walk, the ‘atoms’ keep step, they are in phase with their neighbours. For the incoherent walk, the ‘atoms’ move in all directions, out of phase with each other.

dispersions are characterised by the type of atomic motion. For acoustic phonons there is coherent motion of the atoms out of their equilibrium positions. Whereas in optical phonons there is out of phase (incoherent) motion, one atom moving to the left, and its neighbour to the right. See Figure 4 for a visual depiction of coherence.

For typical thermal energies from room temperature to roughly the melting point of most semiconductors (approximately 1300K), we can neglect the optical phonons. We can do this because the lower energy acoustic phonons are dominant. This is seen in the Bose-Einstein distribution Figure 3, where phonons with frequency at and above approximately 15THz are optical. There is a much higher probability for phonons at lower frequencies and therefore a much higher occupancy.

2.3 Debye Isotropic Continuum Model

By assuming that we only have acoustic phonons, we are well justified in using the approximations in the Debye model, greatly simplifying the theory.

Our first approximation is that our nanocomposites form an *isotropic continuum*, which means that the sample size is much larger than the typical phonon wavelength and it is the same everywhere. This is a valid assumption, as long as our nanocomposite structure is regular and periodic and we have macroscopic samples.

With this approximation, we can assume that our nanocomposite has translational symmetry. This enables us to invoke Bloch's theorem [13], which means for our phonons, all unit cells of the crystal lattice are equivalent. Mathematically this is $f(\mathbf{q}) = f(\mathbf{q} + \mathbf{T})$, where \mathbf{q} is the wavevector and \mathbf{T} is a lattice translation vector. The result of this is that if we can calculate properties for one unit cell, we have solved the entire crystal structure, monumentally simplifying the theory.

Our second approximation is that our unit cells can be modelled as a Debye spheres [13]. This means that for a given unit cell, the wavevector \mathbf{q} will be the same in all directions, forming a sphere. This is a good approximation, with a typical error of just 5-10% [14]. Using this we can easily derive the density of states, which can be used to calculate the specific heat, phonon mean free path and ultimately the phonon thermal conductivity.

Assumptions

- Optical phonons can be neglected up to 1300K
- Our nanocomposite structure is an isotropic continuum
- Unit cells can be modelled as Debye spheres

2.4 Phonon Thermal Conductivity

Crucial to the EMA model [11] used in our nanocomposite theory, is the bulk phonon thermal conductivity k_{ph} . To find k_{ph} , we can model our phononic system as an ideal monatomic gas and use the kinetic theory of gases to describe their motion, leading to [13]

$$k = \frac{1}{3} \int C(\omega) \nu(\omega) \Lambda(\omega) d\omega \approx \frac{1}{3} C \nu \Lambda \quad (3)$$

where C is the volumetric specific heat, ν is the phonon group velocity and Λ is the phonon mean free path.

This can be derived more rigorously using the Boltzmann equation (1). We can inspect a particular region of material, with n as the number of phonons in this region. Phonons can leave this region by two mechanisms, diffusion or decay. Putting this together we get:

$$\frac{d\langle n \rangle}{dt} = \left(\frac{\partial \langle n \rangle}{\partial t} \right)_{\text{diffusion}} + \left(\frac{\partial \langle n \rangle}{\partial t} \right)_{\text{decay}} \quad (4)$$

which, with some effort [14], leads to:

$$k = \frac{1}{3} \sum_{\mathbf{q}, \mathbf{s}} C(\mathbf{q}, \mathbf{s}) \nu(\mathbf{q}, \mathbf{s}) \Lambda(\mathbf{q}, \mathbf{s}) \quad (5)$$

where \mathbf{q} and \mathbf{s} are the wavevector and polarisation of the phonons.

We used expression (3), as an analytical approximation to expression (5). Later, using these analytical results as a guide, we found a numerical solution to (5).

For us to be able to use expression (3) we must describe the phonons as a ideal monoatomic gas, so we make the following assumptions:

Assumptions

- The phonons are much smaller than the sample they exist in

- The phonons are numerous, so a statistical treatment can be used
- The phonons are in constant, random and rapid motion
- Phonon collisions are perfectly elastic
- Other than collisions, there are no interactions between phonons

Despite these many assumptions, our numerical analysis of equation (5) showed good agreement with the analytical results of equation (3). It therefore follows that phonons are well described as an ideal monoatomic gas.

So we have derived an expression for k and defined the parameters needed for the phononic contribution to our thermoelectric nanocomposite. We must now derive the last pieces of the jigsaw; σ , S and k_{el} .

An important quantity in defining σ , S and k_{el} is the Fermi level E_F . The Fermi level defines the highest occupied energy state of a system of electrons, at a given temperature T [13]. It is important in determining the number of electrons available for electrical conduction. So it's a good place to start the discussion.

2.5 Fermi Level

We are familiar with the derivation of the *Fermi energy* [13], which is based upon Pauli's exclusion principle and defines the highest energy electron state at absolute zero. It is a relevant quantity in all materials for calculating solid state properties. However, with the small band gap of semiconductors used in thermoelectrics, additional temperature effects have to be accounted for.

The Fermi level for an intrinsic semiconductor can be defined as [15]:

$$E_F = E_g + k_B T \ln \left(\frac{m_h^*}{m_e^*} \right)^{\frac{3}{4}} \quad (6)$$

where E_g is the band gap defined as $\frac{1}{2}(E_v + E_c)$, E_v, E_c are the valence and conduction band edges and m_e^*, m_h^* are the effective masses of electrons and holes.

For an extrinsic semiconductor the donor or acceptor atoms increase the Fermi level, but this is only significant at temperatures below a certain threshold. We must add an additional component to our intrinsic expression to account for this. This is well justified in McKelvey [15], for brevity I will simply state the expression below:

$$E_F = E_g + k_B T \ln \left(\frac{m_h^*}{m_e^*} \right)^{\frac{3}{4}} + k_B T \sinh^{-1} \left(\frac{N_d - N_a}{2\sqrt{U_c U_v} e^{\frac{-E_g}{2k_B T}}} \right) \quad (7)$$

where N_d, N_a are the concentration of donor/acceptor atoms and U_c, U_v are the effective density of states for the conduction/valence bands.

This expression is used in the derivation of all the electrical properties and it's an essential ingredient for the discussion on thermoelectricity in Section 3.1. See Figure 5 for a comparison plot between the extrinsic (7) and intrinsic equations (6) for an n-type SiGe semiconductor.

Assumptions

- Energy bands are parabolic and can be linearised at band edges
- The effective masses of holes and electrons do not vary with temperature and can be resolved to a single parameter
- The density of donor or acceptor atoms does not vary with temperature, pressure or spatial location

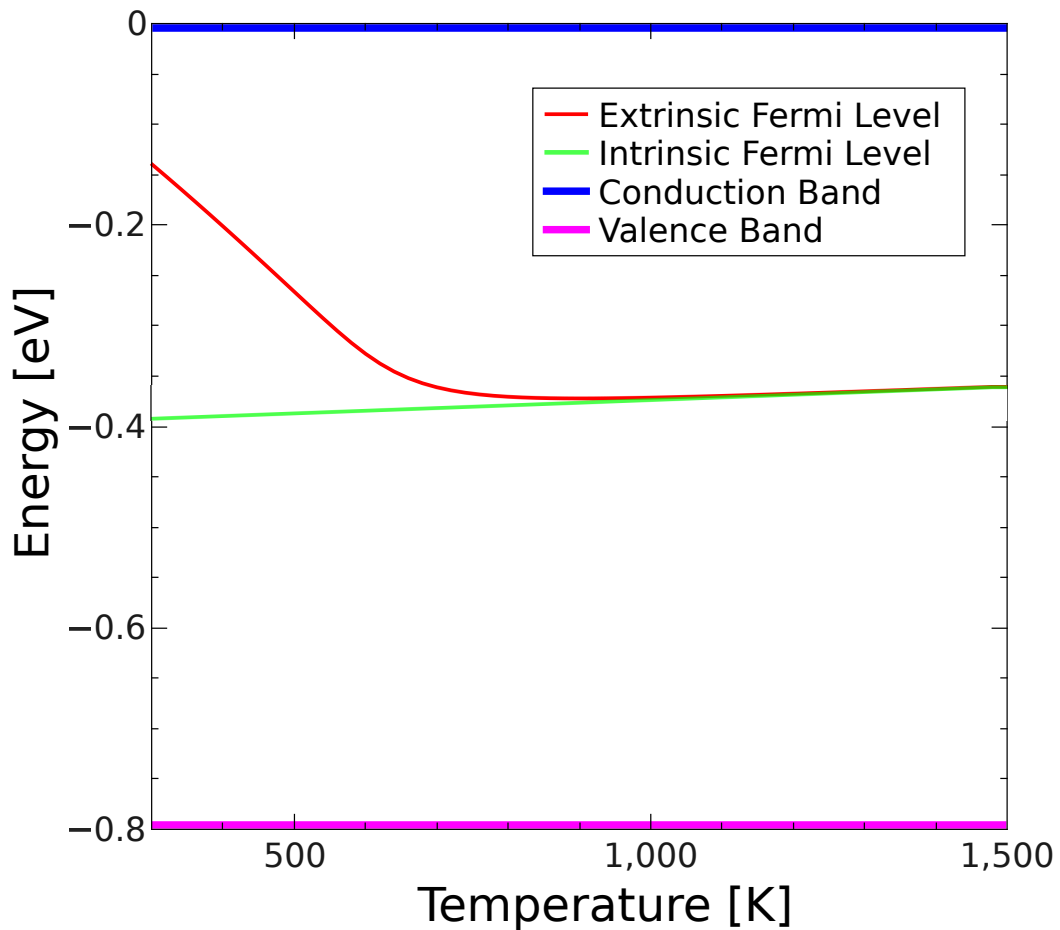


Figure 5: Extrinsic Fermi level (7) and intrinsic Fermi level (6) *versus* energy for a n-type SiGe semiconductor. The extrinsic component of the Fermi level dominates over the intrinsic component from room temperature to 800K. Above 800K donor atoms have lost all their electrons and they no longer play a role in determining the Fermi level.

2.6 Electrical Conductivity

The goal of our nanocomposite structuring is to enhance the heat to electric conversion efficiency and a vital component of that is the electrical conductivity σ . Kittel [13] uses kinetic theory arguments similar to those in Section 2.4 to define a simple expression for electrical conductivity:

$$\sigma = ne\mu \quad (8)$$

where n is the number of charge carriers available for conduction, e is the elementary charge and μ is the carrier mobility.

n can be defined in terms of the density of states $g(\mathbf{q})$ and the distribution of charge carriers $f(\mathbf{q})$ as follows [13]:

$$n = \int g(\mathbf{q})f(\mathbf{q})dE = \frac{1}{6\pi^2} \left(\frac{2m_c k_B T}{\hbar^2} \right)^{\frac{3}{2}} F_{\frac{1}{2}}(\eta) \quad (9)$$

where E is the energy range of interest, m_c is the mass of the charge carrier, T and η is the reduced Fermi level equal to $\frac{E_f}{k_B T}$

This expression, along with a similar expression for mobility μ [13] result in several non-analytical integrals called the *Fermi-Dirac integrals*:

$$F_r(\eta) = \exp(\eta) \int_0^\infty x^\eta \exp(-x) dx \quad (10)$$

These Fermi integrals can be approximated for a high temperature limit, defined as $E_c - E_f \gg k_B T$, where E_c, E_f are the conduction band and Fermi level. This approximation is known as the *Boltzmann approximation* [13] and leads to the following expression for the Fermi integrals:

$$F_r(\eta) \approx \exp(\eta)\Gamma(r+1) \quad (11)$$

where Γ is the gamma function. We use this expression to approximate Fermi integrals for all our analytical results. It is accurate for large negative values of η and 95% accurate when $\eta = -2$ [16]. For our analysis $\eta < -2$, we can therefore be confident in this approximation.

Using this approximation for the n and μ expressions (9) and substituting into equation (8) we get our final expression [16]:

$$\sigma = 2e(2\pi k_B Th^{-2})^{\frac{3}{2}}(m_e^* m_h^*)^{\frac{3}{4}}(\mu_e + \mu_h) \exp\left(\frac{-E_g}{2k_B T}\right) \quad (12)$$

where m_e^*, m_h^* are the effective masses of electrons and holes and μ_e, μ_h are the mobilities of electrons and holes.

For our final results we evaluate the Fermi integrals numerically using Simpson's rule, a simple extension of the trapezium rule, which is much more accurate than our analytical approximations [16]:

$$\int_a^b f(x)dx \approx \frac{b-a}{6} \left[f(a) + 4f\left(\frac{a+b}{2}\right) + f(b) \right] \quad (13)$$

Assumptions

- Electrons can be described by the kinetic theory of gases
- Boltzmann approximation applies - $E_c - E_f \gg k_B T$
- Effective masses and mobilities do not vary with temperature

2.7 Electrical Thermal Conductivity

The electrical conductivity σ derived in the previous section describes how easily electrons can flow through a material. As you might expect, the thermal conductivity due to electrons k_{el} is closely tied to this. All we must define is the amount of heat energy each electron carries.

Following Drabble [16] we can define an expression for the electrical thermal conductivity k_{el} in terms of σ as follows:

$$\frac{k_{el}}{\sigma T} = \frac{k_B^2}{e^2} \left(\frac{(p + \frac{7}{2})(p + \frac{3}{2})F_{(p+5/2)}F_{(p+1/2)} - (p + \frac{5}{2})^2 F_{(p+3/2)}^2}{(p + \frac{3}{2})^2 F_{(p+1/2)}^2} \right) \quad (14)$$

where p is the energy power law for electron-phonon scattering and $F_{(p+1/2)}$ is the Fermi integral for a given p .

As described in Section 2.2, we assume that acoustic phonons are dominant, thus acoustic electron-phonon scattering is also dominant. We therefore consider only one type of scattering and take $p = -\frac{1}{2}$ as its energy power law value [16].

Using the Fermi integral approximation (11) and $p = -\frac{1}{2}$, equation (14) simplifys to:

$$k_{el} = 2\sigma T k_B^2 / e^2 \quad (15)$$

Which is the expression used in our analytical results, with the Fermi integrals of equation (14) solved numerically using (13), in our final results.

III Specific Theory

Now that we have the background theory we can understand the specific theories that apply to our zero-dimensional nanocomposite thermoelectric.

3.1 Thermoelectric Effect & Seebeck Coefficient

In 1821, Thomas Seebeck discovered that circuit made from two dissimilar metals, with junctions at different temperatures would deflect a compass magnet (Figure 6), he had discovered thermoelectricity. The temperature gradient ∇T between the junctions generates an electromotive force:

$$\mathbf{E}_{\text{emf}} = -S\nabla T \quad (16)$$

where S is the Seebeck coefficient, defined as the induced voltage per unit temperature, mathematically $\Delta S = \frac{\Delta V}{\Delta T}$ [1]. A temperature gradient produces an electromotive force gradient, which in turn produces a current density gradient described macroscopically by a modified Ohm's law [13]:

$$\mathbf{J} = \sigma(-\nabla V - S\nabla T) \quad (17)$$

where \mathbf{J} and σ are the current density and electrical conductivity at a given location in the material and ∇T and ∇V are the temperature and resultant voltage gradients across the material. If we were to repeat the experiment conducted by Seebeck (Figure 6), but instead of a compass we use a voltmeter, we could find σ and V . Assuming a steady state system, i.e. the current and current density are zero $I = \mathbf{J} = 0$, we could experimentally determine the Seebeck coefficient.

Similar to the derivation of the electrical thermal conductivity k_{el} in Section 2.7, we can theoretically define the Seebeck coefficient in terms of the reduced Fermi level η [16]:

$$S = \frac{k_B}{e} \left(\eta - \frac{(p + \frac{5}{2})F_{p+3/2}}{(p + \frac{3}{2})F_{p+1/2}} \right) \quad (18)$$

As is done in Section 2.7, we use the Fermi integral approximation (11) and set $p = -\frac{1}{2}$, simplifying the expression to:

$$S = \frac{k_B}{e} \left(\frac{E_F}{k_B T} - 2 \right) \quad (19)$$

Again we use this analytical approximation as a guide to our numerical solution of expression (18), using Simpson's rule (13) in our final results.

So we can define the Seebeck coefficient that gives the voltage induced from a thermal gradient. But if we want to find the heat to electric conversion efficiency, there are other variables to consider. What are these variables and how do they interact?

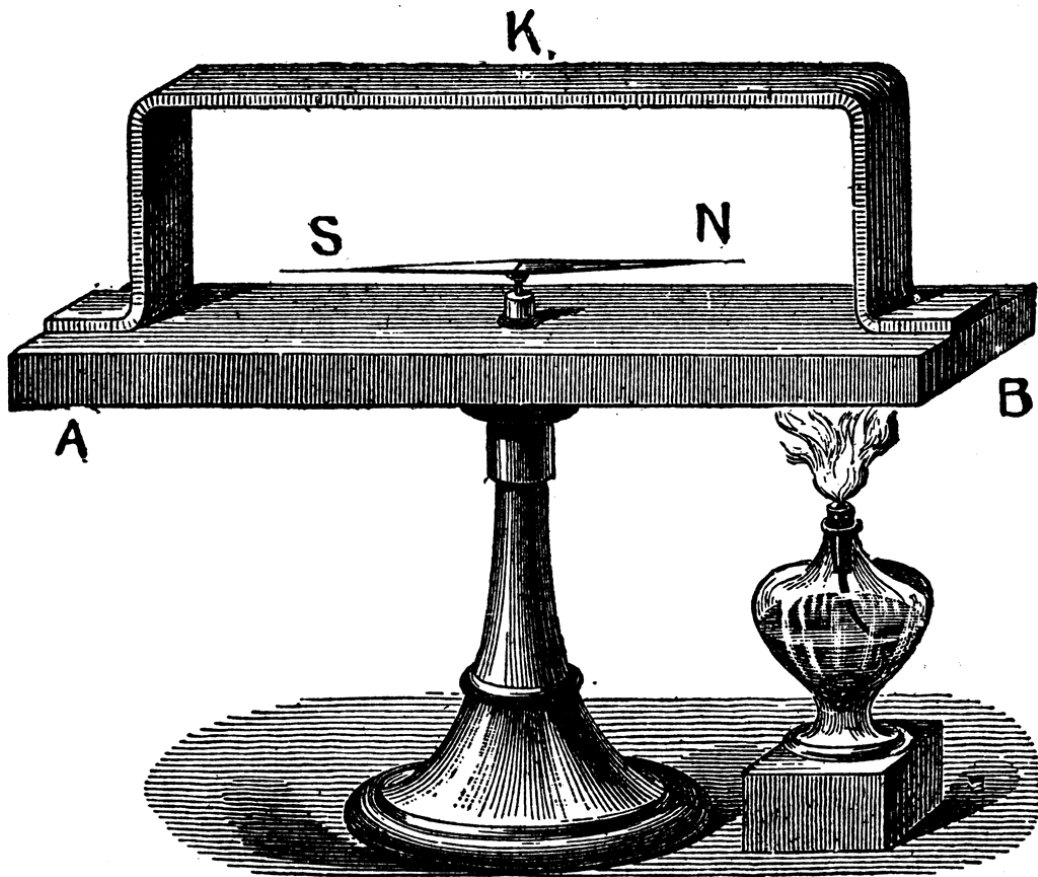


Figure 6: Thomas Seebeck's original thermoelectricity experiment diagram [17]. A compass needle lies on top of one metal, underneath a bridge of a different metal K , connected by two junctions and heated at one side. The heat produces a thermoelectric current in the junctions, creating a weak magnetic field, deflecting the compass needle. Measuring the voltage and resistance between K and the centre of the compass would allow the Seebeck coefficient S to be determined.

3.2 Thermoelectric Efficiency

Thermoelectric efficiency is best defined by the dimensionless parameter ZT . The total heat to electric efficiency is a function of (ZT, T_h, T_c) , where Z is the figure of merit, $T = \frac{1}{2}(T_h + T_c)$ and T_h, T_c are the temperatures at the hot and cold junctions. ZT is defined as [1]:

$$ZT = \frac{S^2\sigma T}{k_{el} + k_{ph}} \quad (20)$$

where S is the Seebeck coefficient, σ is electrical conductivity, k_{el} and k_{ph} are the thermal conductivity due to electrons and phonons respectively.

Important points to note about ZT are that it is proportional to thermal efficiency, is increased by a reduction in thermal conductivity and it depends on the square of the Seebeck coefficient. Figure 1 in Section 1.2 demonstrates the interaction between these variables .

So we now have the final expression we want to evaluate, equation (20) and have defined for bulk materials the different variables used. We now need to consider what exactly are nanocomposites and how do they effect the bulk material properties.

3.3 Nanocomposites

Composites are combinations of two or more materials, forming a new structure with significantly different physical or chemical properties than its constituent parts. In a similar way, nanocomposites are the structuring of multiple materials, but at the nanoscale. As our nanocomposites are at a comparable size to the crystal lattices of their constituent materials, we can view nanocomposites as artificial defects in a larger crystal lattice.

A simple example of a 2D nanocomposite, a copper-graphene superlattice, is shown in Figure 7. One layer of the superlattice in bulk form would be an ordinary 3D crystal structure. By constraining the layer thickness, we introduce a boundary defect. The periodic array of these boundary defects forms a new artificial 3D crystal, which we define as the superlattice. Other nanocomposite structures are shown in Figure 8 and a STEM in Figure 9.

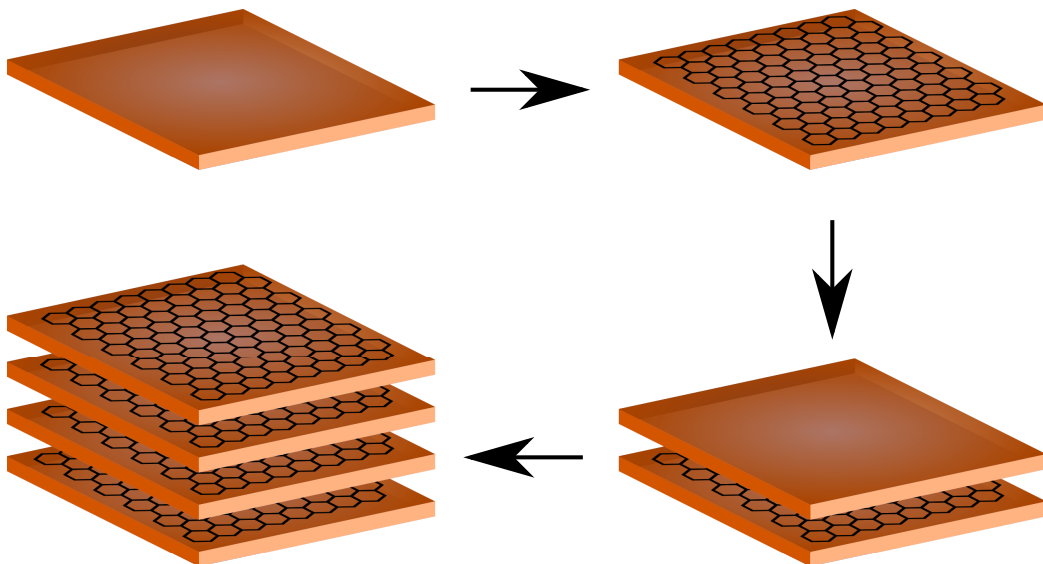


Figure 7: Superlattice of graphene and copper. Alternate layers of nanoscale copper and graphene are sandwiched together to form an artificial 3D crystal, which has distinct properties from the individual layers.

From a qualitative understanding of nanocomposites, there must be strong boundary and interface effects; by definition they contain numerous transitions between two or more materials, where each transition forms a new interface. Therefore a thorough understanding of how these interfaces affect the propagation of phonons and electrons is required, to work out the effects of nanocomposite structuring on thermoelectricity.

As discussed in Section 1.2, we decided to ignore the electron and only consider the phonon effects. This is justified by the fact that in our structure we consider 10nm nanoparticles, much smaller than the electron wavelength. Therefore any effects that are present are likely to be negligible; a 10nm nanoparticle is much more likely to scatter a phonon than an electron.

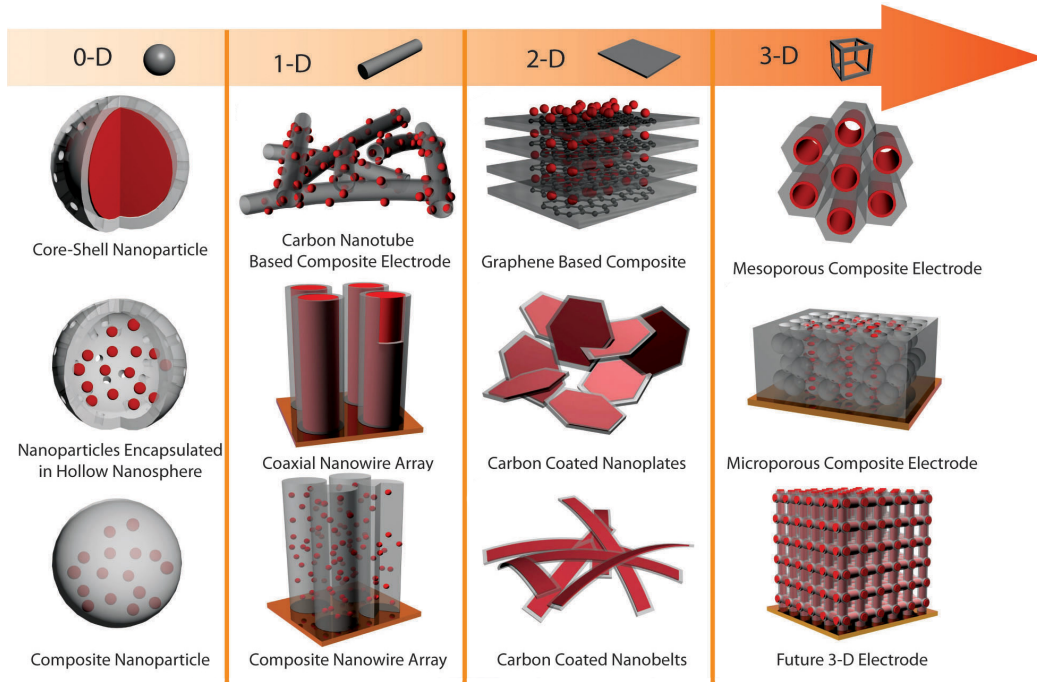


Figure 8: A range of nanocomposite structures, arranged in increasing dimensionality. Our chosen system is a *composite nanoparticle* [10].

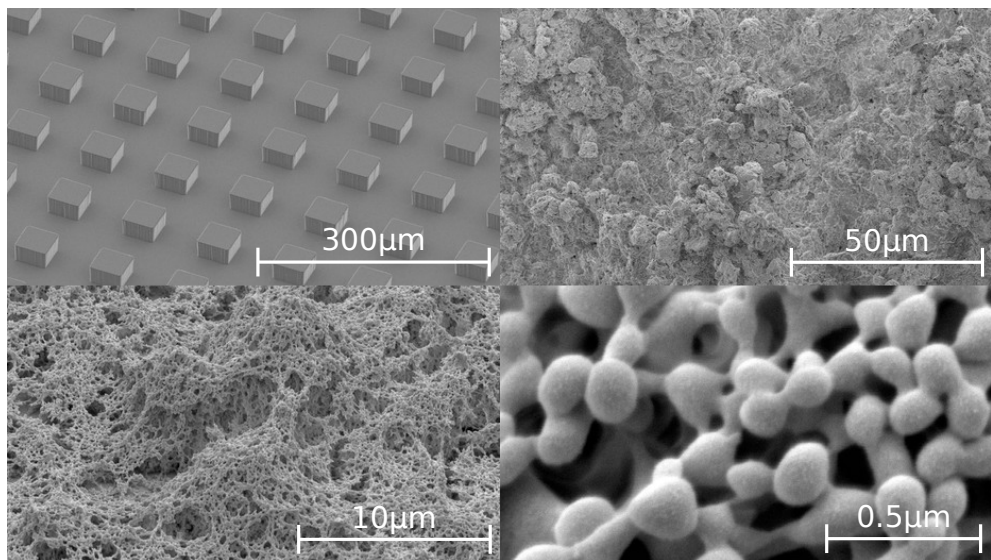


Figure 9: STEM of a recently fabricated 3D nanocomposite structure [8].

3.4 Effective Medium Approximation

The effective medium approximation (EMA) considers a homogeneous host material with a phonon thermal conductivity k_h , that is regularly perturbed by an interface resistance R and separate phonon thermal conductivity k_p , which is then averaged over a relevant length scale d . For spherical particles the theory takes the following form [11]:

$$\frac{k_e}{k_h} = \frac{k_p(1 + 2\alpha) + 2k_h + 2\varphi[k_p(1 - \alpha) - k_h]}{k_p(1 + 2\alpha) + 2k_h - \varphi[k_p(1 - \alpha) - k_h]} \quad (21)$$

where k_e is the effective composite thermal conductivity, k_h is the host material thermal conductivity, k_p is the particle thermal conductivity, φ is the volume fraction of nanoparticle inclusions and $\alpha = R/(d/2)$, where R is the thermal boundary resistance and d is the diameter of the spherical particles.

The crucial problem with this theory in application to nanocomposites, is that it fails to account for the increased scattering in and around particles. The modified-EMA (mEMA) [18] introduces additional terms into the mean free path of the thermal conductivity expressions to address this:

$$\Lambda_{COLL} = \frac{4a^3}{\pi d^2} \quad (22)$$

where a is the unit cell effective length defined from the density of nanoparticles $n = 1/a^3$, d is the diameter of the nanoparticles.

Using these modifications in the equations derived for phonon thermal conductivity in Section 2.4, we can define a new effective k_p and k_h , which we then substitute back into (21). This additional scattering is significant and it substantially lowers the phonon thermal conductivity [18].

Studying the mEMA, we found that the smallest possible particles would give the lowest phonon thermal conductivity. We decided upon 10nm as our final particle size, as it is comparable with the phonon wavelength. If we used smaller particles, then the whole idea of a phonon breaks down.

IV Results and Analysis

To get our final results, we computed each component of the ZT expression (20) in Fortran, using materials data from Springer [19]. We used Simpson's rule (13) to compute any integrals, checking results with our analytical approximations. We took a nanocomposite of 10nm silicon spheres, at near maximum filling, which roughly corresponds to a ratio of 70-30 GeSi. See Figure 2 in Section 1.2 for a diagram of this structure.

Figure 10 compares 4 different nanocomposite phonon thermal conductivity models. It shows the progressive decrease in phonon thermal conductivity, as more nanostructuring effects are considered in the theory. The *Specular EMA* [20] is not mentioned in the report, since the derivation was lengthy and it did not produce significantly different results from the mEMA. The weighted average is calculated from the bulk thermal conductivities of the two materials, considering no nanocomposite effects.

EMA models show a surprisingly constant temperature dependence. This is because of the dominance of diffuse phonon scattering at particle interfaces. All other phonon thermal conductivity contributions become negligible in comparison.

During the calculation of Figure 10, it was clear that maximising the particles surface area per unit volume (interface density) is key to minimising the phonon thermal conductivity. It appears to have no effect on the electrical transport properties and maximises phonon scattering. We chose the 10nm particle size from this analysis.

Figure 11 shows the final ZT values for our nanocomposite structure. Comparing this to historical SiGe thermoelectric results in Figure 12, we can see that over the usable temperature range of 700-1200K, the nanostructuring has increased ZT roughly 4x . The primary mechanism for this is likely to be phonon scattering in between nanoparticles, but further investigation is required to verify this.

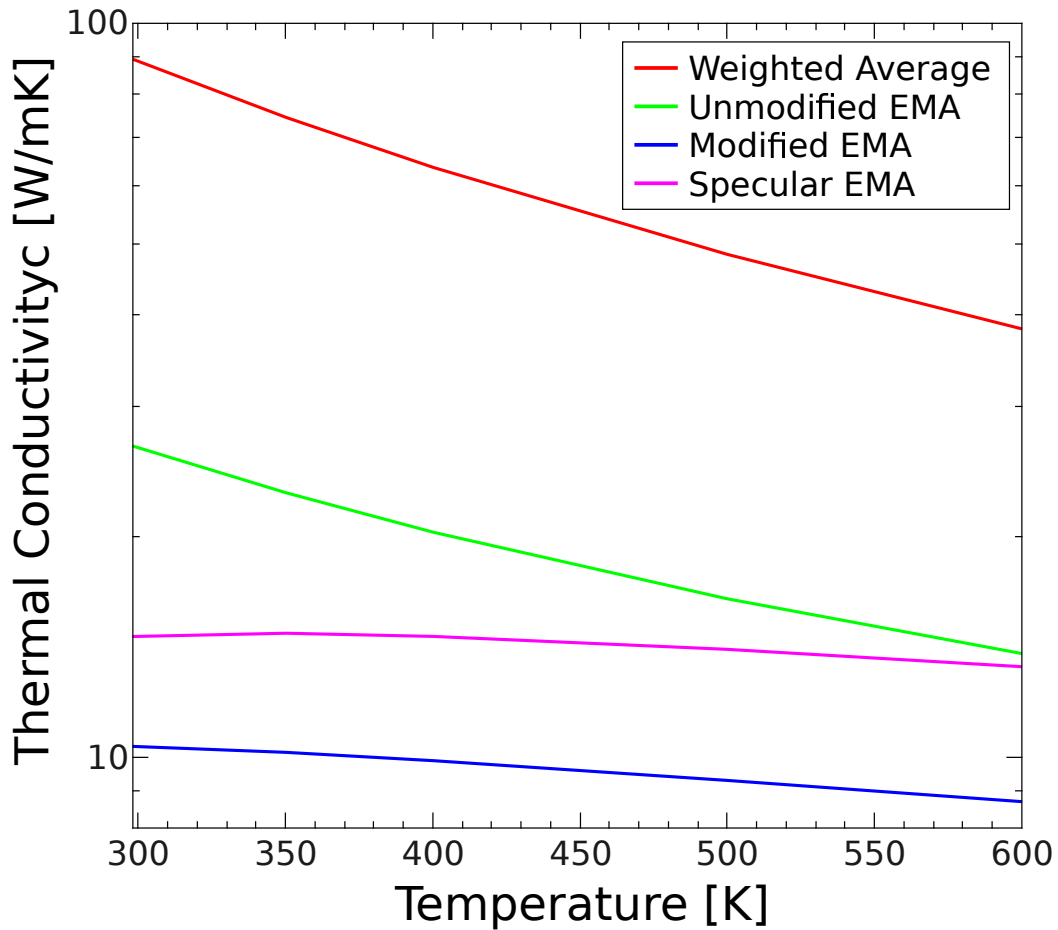


Figure 10: A comparison between 4 different phonon thermal conductivity models for a 70-30 GeSi nanocomposite. The *Modified EMA* was chosen for the final results and lowers the conductivity approximately 10x . The *Weighted Average* considers no nanocomposite effects. The *Unmodified EMA* [11] ignores increased scattering due to nanoscale structures. The *Modified EMA* [18] considers increased diffuse phonon scattering at nanoparticle interfaces. The *Specular EMA* [20] considers both diffuse and specular phonon scattering at nanoparticle interfaces.

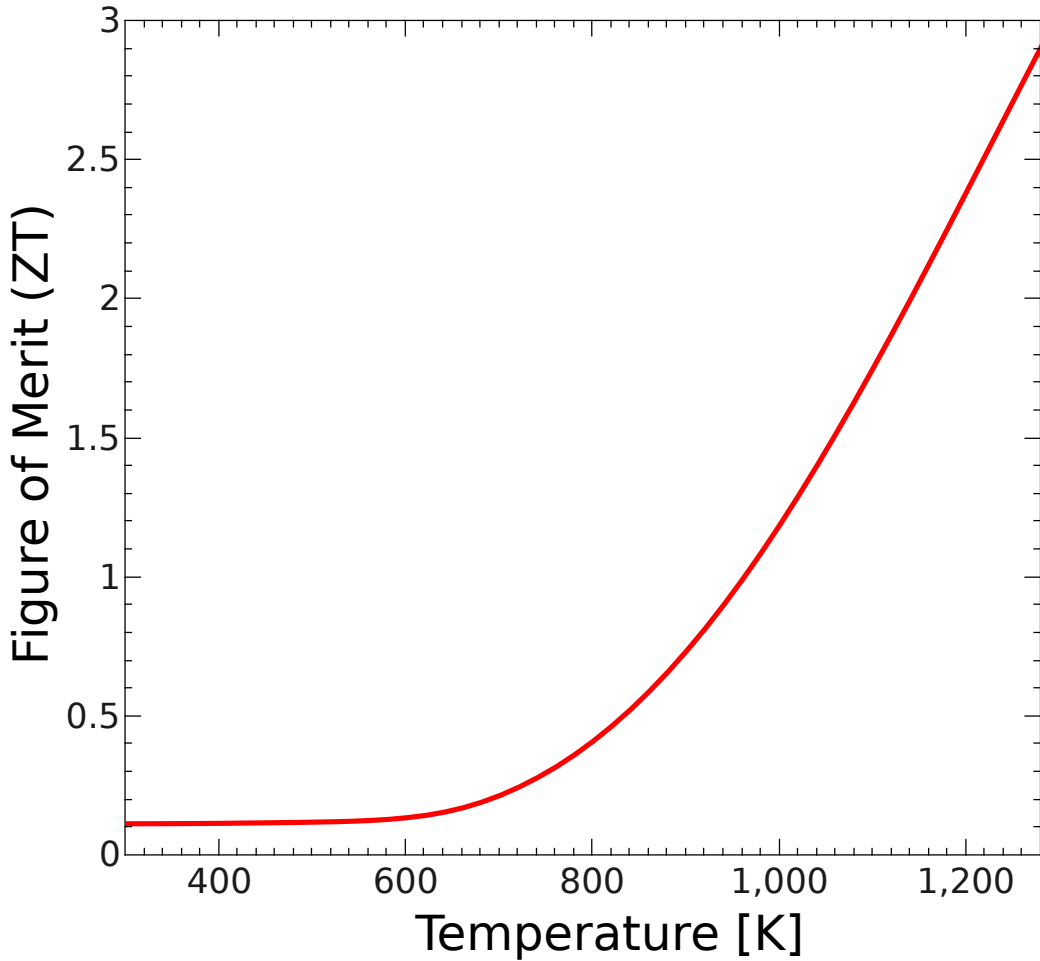


Figure 11: ZT versus temperature for a 70-30 GeSi zero-dimensional nanocomposite, using bulk electrical transport theory and modified EMA [18] phonon thermal conductivity theory. As temperature increases, the decreasing phonon thermal conductivity greatly enhances ZT . Comparing to historical SiGe thermoelectric results in Figure 12, we see that ZT has increased roughly 4x over the usable temperature range (700-1200K).

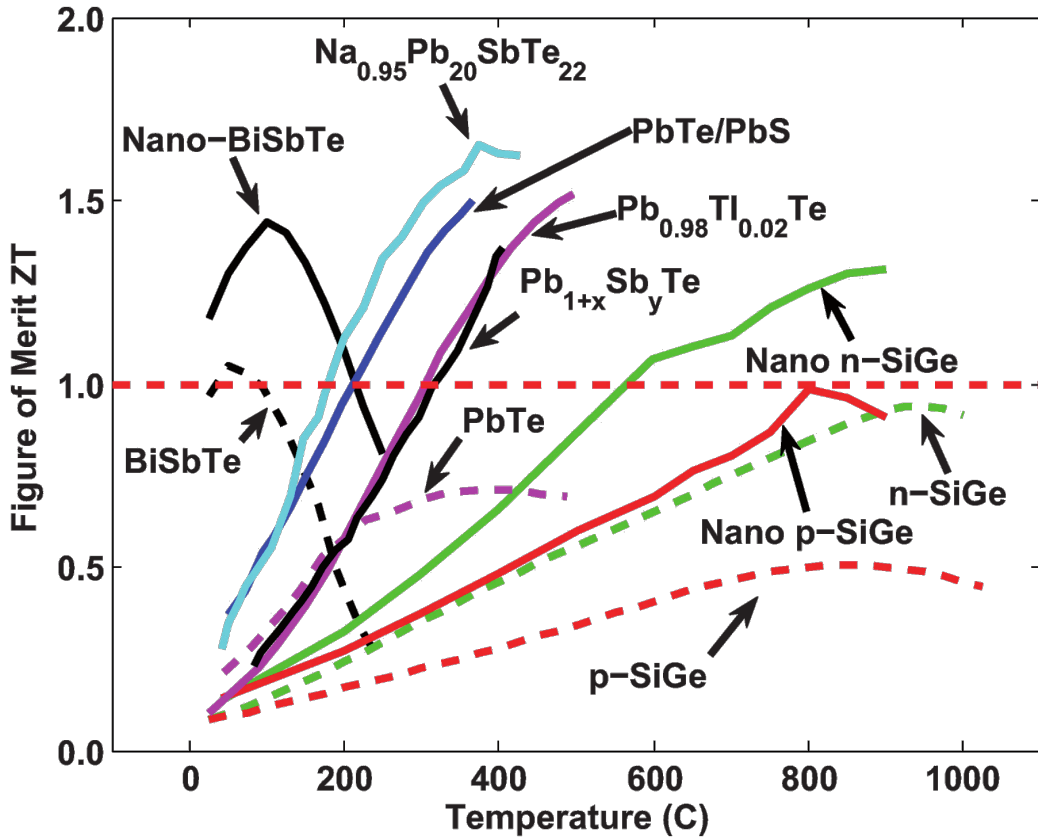


Figure 12: Thermoelectric figure of merit ZT against temperature for nanocomposite and bulk thermoelectrics [8]. The dashed lines represent previous generation bulk thermoelectric materials, the solid lines represent recent nanocomposite thermoelectrics.

V Conclusion and Future Work

We have derived expressions for the electrical and thermal conductivities of a 10nm 30-70 SiGe zero-dimensional nanocomposite. We utilised an effective medium approximation to calculate phonon thermal conductivity and find that nanostructuring greatly reduces this quantity. We find that phonon thermal conductivity is minimised for spheres of 10nm diameter. Further investigation may find that smaller spheres are possible and give an even greater decrease in the phonon thermal conductivity.

Combining all our results, we find that a 10nm SiGe zero-dimensional nanocomposite increases the thermoelectric efficiency approximately 4x compared to bulk. This gives good indication that further theoretical and experimental research should be conducted in this field.

5.1 Future Work

- Create a nanocomposite theory of electrical transport
- Find temperature dependent material properties (band gap etc.) and calculate ZT
- Derive an expression for the total efficiency of a thermoelectric generator. Is the ZT improvement translatable to a real world application?
- Investigate the effects of non-spherical particle shapes. Particularly a tessellating 3D shape, to maximise interface density
- Derive a non-phonon based theory to investigate nanoparticle sizes smaller than 10nm

5.2 Online repository

Private access due to the University of Exeter's intellectual property rules.

<https://github.com/kahlos/thermoelectrics>

References

- [1] D. M. Rowe, *Modern Thermoelectrics*, September 1983, Holt-Technology, ISBN:978-0835945936 **Page 12**
- [2] M. L. Baglione, *Development of System Analysis Methodologies and Tools for Modeling and Optimizing Vehicle System Efficiency*, 2007, University of Michigan, DOI:2027.42/57640 **Pages 52-54**
- [3] R. Venkatasubramanian *et al.*, *Thin-film thermoelectric devices with high room-temperature figures of merit*, October 2001, Nature, vol. 413, pp. 597-602, DOI:10.1038/35098012
- [4] W. Liu *et al.*, *Recent advances in thermoelectric nanocomposites*, January 2012, Nano Energy, vol. 1, iss. 1, pp. 42-56, DOI:10.1016/j.nanoen.2011.10.001
- [5] D. Kraemer *et al.*, *High-performance flat-panel solar thermoelectric generators with high thermal concentration*, May 2011, Nature Materials 10, pp. 532-538, DOI:10.1038/NMAT3013
- [6] X. Liu *et al.*, *A case study on compatibility of automotive exhaust thermoelectric generation system, catalytic converter and muffler*, March 2014, Case Studies in Thermal Engineering, vol. 2, pp. 62-66, DOI:10.1016/j.csite.2014.01.002
- [7] L. E. Bell, *Cooling, Heating, Generating Power, and Recovering Waste Heat with Thermoelectric Systems*, September 2008, Science 12, vol. 321, no. 5895, pp. 1457-1461, DOI:10.1126/science.1158899
- [8] A. J. Minnich *et al.*, *Bulk nanostructured thermoelectric materials: current research and future prospects*, Februry 2009, Energy Environ. Sci. 2, pp. 466-479, DOI:10.1039/B822664B
- [9] G. A. Slack, ed. D. M. Rowe, *CRC Handbook of Thermoelectrics*, 1995, CRC Press, ISBN:978-0849301469 **Pages 407-440**
- [10] L. D. Hicks, M. S. Dresselhaus, *Thermoelectric figure of merit of a one-dimensional conductor*, June 1993, Phys. Rev. B 47, 16631 DOI:10.1103/PhysRevB.47.16631

- [11] C. Nan *et al.*, *Effective thermal conductivity of particulate composites with interfacial thermal resistance*, February 1997, Journal of Applied Physics 81, pp. 6692-6699, DOI:10.1063/1.365209
- [12] L. Braginsky *et al.*, *High-temperature phonon thermal conductivity of nanostructures*, October 2002, Physical Review B 66, 134203, DOI:10.1103/PhysRevB.66.134203
- [13] C. Kittel, *Introduction to Solid State Physics*, 8th Ed., November 2004, John Wiley & Sons, ISBN:978-0471415268
- [14] G.P Srivastava, *The Physics of Phonons*, January 1990, CRC Press, ISBN:978-0852741535
- [15] J. P. McKelvey, *Solid State and Semiconductor Physics*, 1966, Harper & Row, ISBN:978-0898743968 **Pages 262-276**
- [16] J. R. Drabble, H. J. Goldsmid, *Thermal Conduction in Semiconductors*, 1961, Pergamon Press, DOI:10.1002/zfch.19630030421 **Pages 109-111**
- [17] http://www/etc.usf.edu/clipart/35600/35659/seebbeck_35659_1g.gif, 24 November 2013
- [18] A. Minnich, G. Chen, *Modified effective medium formulation for the thermal conductivity of nanocomposites*, August 2007, Appl. Phys. Lett. 91, 073105, DOI:10.1063/1.2771040
- [19] Springer, *Springer Handbook of Condensed Matter and Materials Data*, 2005, ISBN:978-3540443766
- [20] A. Behrang *et al.*, *Influence of particle-matrix interface, temperature, and agglomeration on heat conduction in dispersions*, July 2013, Journal of Applied Physics 114, 014305, DOI:10.1063/1.365209

Appendix

A Tools and Software

- Github - An online version control repository
- QtiPlot - Plotting graphs and quick checks of results
- Fortran - Programming computational analysis
- LaTeX - Typesetting this document

B Physical Data

All physical constants used were from the CODATA Recommended Values of the Fundamental Physical Constants 2010.

<http://www.physics.nist.gov/Constants>

All materials data were sourced from the *Springer Handbook of Condensed Matter and Materials Data* [19].